

# Influence of DMPS on the water retention capacity of electroporated *stratum corneum*: ATR-FTIR study

Maria Sckolnick, Sek-Wen Hui, Arindam Sen\*

Membrane Biophysics Laboratory, Roswell Park Cancer Institute, Elm & Carlton Streets, Buffalo, NY 14263, USA

Received 26 June 2007; received in revised form 6 August 2007; accepted 22 August 2007

Available online 26 August 2007

## Abstract

Anionic lipids like phosphatidylserine are known to significantly enhance electroporation mediated transepidermal transport of polar solutes of molecular weights up to 10 kDa. The underlying mechanism of the effect of anionic lipids on transdermal transport is not fully understood. The main barrier to transdermal transport lies within the intercellular lipid matrix (ILM) of the *stratum corneum* (SC) and our previous studies indicate that dimyristoyl phosphatidylserine (DMPS) can perturb the packing of this lipid matrix. Here we report on our investigation on water retention in the SC following electroporation in the presence and the absence of DMPS. The water content in the outer most layers of the SC of full thickness porcine skin was determined using ATR-FTIR-spectroscopy. The results show that in the presence of DMPS, the SC remains in a state of enhanced hydration for longer periods after electroporation. This increase in water retention in the SC by DMPS is likely to play an important role in trans-epidermal transport, since improved hydration of the skin barrier can be expected to increase the partitioning of polar solutes and possibly the permeability.

© 2007 Elsevier B.V. All rights reserved.

**Keywords:** Porcine skin; Stratum corneum; Hydration; Water content; Transdermal transport; Anionic lipids; Dimyristoyl phosphatidylserine; Electroporation; Infrared spectroscopy; ATR-FTIR

## 1. Introduction

Transdermal drug delivery, an attractive alternative to conventional drug delivery methods, has proven difficult for hydrophilic drugs so far. The main barrier to transdermal transport lies in the *stratum corneum*. All molecules passing through the skin have to traverse the intercellular lipid matrix (ILM), a continuous structure of densely packed, saturated lipids with little hydration. This hydrophobic, highly ordered environment has great resistance to the diffusion and partitioning of polar solutes. Water is a known transdermal transport enhancer and increased hydration has been shown to correlate with transdermal transport enhancement of hydrophilic molecules (Cronin and Stoughton, 1962; Scheuplein and Ross, 1974). It has been suggested that high water contents compromise the SC structure and lead to the formation of water pools in the ILM (Warner et al., 2003). Improved partitioning of polar drugs into the more

hydrophilic milieu may also play a role. Hydration of the SC can be improved by occlusion (Blank, 1951), several chemicals, e.g. components of the “natural moisturizing factor” such as pyrrolidones and urea (Feldmann and Maibach, 1974; Walters, 1989; Williams, 1995) as well as the application of a low or high voltage potential (Jadoul et al., 1996, 1999).

Our group has shown that electroporation in conjunction with anionic phospholipids can significantly enhance the post-pulse epidermal permeability for small polar solutes (Sen et al., 2002a). The transepidermal transport of dextran (4 kDa) and insulin (6 kDa) was shown to be increased 80-fold (Sen et al., 2002b) and 20-fold (Sen et al., 2002c), respectively. Saturated phospholipids, in particular 1,2-dimyristoyl-*sn*-glycero-3-[phospho-L-serine] (DMPS), proved to be much more effective than unsaturated phospholipids such as 1,2-dioleoyl-*sn*-glycero-3-[phospho-L-serine] (DOPS) (Sen et al., 2002b,c).

The mechanism of this enhancement is currently being investigated and we have found that incorporation of DMPS into ILM models reduces their lipid packing density and increased hydration as reflected in increased lamellar repeat spacing in these models (manuscript under preparation).

\* Corresponding author. Tel.: +1 716 845 8911.

E-mail address: [Arindam.sen@roswellpark.org](mailto:Arindam.sen@roswellpark.org) (A. Sen).

The objective of this current study is to test the effect of DMPS on the hydration behavior of skin, we report here on our studies on full thickness porcine skin by Fourier transform infrared spectroscopy (FTIR-spectroscopy). FTIR-spectroscopy is a non-invasive and elegant way to determine the hydration status of the SC. As was shown by Potts et al. (1985), IR-absorbance at the position of the weak combination band near  $2100\text{ cm}^{-1}$  can provide quantitative information on the hydration of skin.

In attenuated total reflectance FTIR-spectroscopy (ATR-FTIR-spectroscopy) the light reflecting off the internal surfaces of an internal-reflection-element, e.g. a silica crystal penetrates a short distance ( $\sim 1\text{ }\mu\text{m}$ ) as an evanescent wave from the surface of the crystal into a skin sample pressed against it. Interaction of this evanescent wave with the surface of the skin, which corresponds to SC tissue, can be detected in the spectrum of the IR-beam that exits the crystal. ATR-FTIR has been applied successfully to determine the hydration of skin in vitro and in vivo by other groups (Edwardson et al., 1991; Jadoul et al., 1996; Potts et al., 1985).

ATR-FTIR is only able to detect surface hydration and furthermore, ATR-FTIR can only be used to determine the hydration status at distinct time points, since the skin has to be pressed onto the crystal, occluding the SC surface. In order to determine the hydration status of an ILM model as a function of time we used transmission FTIR-spectroscopy. The IR-beam in transmission spectroscopy samples the entire thickness of an ILM model filled membrane filter, which is placed against a  $\text{CaF}_2$  crystal.

## 2. Experimental procedures

### 2.1. Full thickness porcine skin

Porcine skin was obtained from the abdomen of experimental animals in the Department of Medicine, State University of New York at Buffalo. Hair and fat were removed from the skin. Pieces were wrapped in aluminum foil and stored at  $-80\text{ }^\circ\text{C}$  until use.

### 2.2. DMPS dispersion

DMPS dispersion was prepared by drying a solution of DMPS in chloroform in a glass vial under a gentle stream of dry  $\text{N}_2$ . Excess solvent was removed in a vacuum desiccator for 1 h. Phosphate-buffered saline (PBS) was added to the dry lipid give a  $4\text{ mg/mL}$  final concentration. The lipid–PBS mixture in the vial was sonicated for about 1 min in a bath type sonicator (Special Ultrasonic Cleaner (Model: G112SP1G, Laboratory Supplies Co. Inc., Hicksville, NY, USA) until all of the lipid were dispersed resulting in a cloudy dispersion.

### 2.3. Transdermal permeabilization

One hour before an experiment, pieces of skin were thawed at room temperature, cut into squares to fit a Franz-type diffusion cell, put on microscope slides with the SC side up and equilibrated for at least 30 min in a 43% relative humidity (RH) chamber containing a saturated potassium carbonate solution

(Greenspan, 1977). We selected 43% RH, because this value falls within the range of typical ambient air RH-values. The skin was then mounted with the SC side up in a Franz-type diffusion cell with platinum wire electrodes. The receptor chamber was filled with PBS. The donor chamber contained  $200\text{ }\mu\text{L}$  of either PBS or DMPS dispersion. Only the skin pieces that had an initial resistance  $R > 5\text{ k}\Omega$  were used. Electroporation was conducted by applying square pulses of  $150\text{ V} \pm 10\%$  at 1 Hz for 60 s using a high voltage pulse generator (Velonex, Model 345, Venus, CA, USA). After electroporation, the donor liquid was removed and the skin surface was rinsed twice with excess PBS. Exposure to PBS or DMPS dispersion during this process lasted 4 min. Following rinsing, excess water was removed from the skin with a piece of filter paper and the skin was put back on the microscope slide in the RH-chamber.

### 2.4. ATR-FTIR measurements

Just before the infrared-spectrum was taken, the piece of skin was trimmed down to the area that had been exposed to the donor liquid during electroporation and placed SC side down on top of a trapezoidal ATR silica crystal. The skin was pressed onto the crystal with a 100 g standard weight. An average of 100 spectra was obtained, baseline-corrected, and processed (Spectrum software, Perkin-Elmer, Boston, MA, USA). For each group between 7 and 9 skin pieces were tested. Student's *t*-test and the *p*-values were determined using Microsoft Excel program.

### 2.5. ILM models

DMPS and cholesterol (Chol) were obtained from Avanti Polar Lipids (Alabaster, AL, USA). Stearic acid (SA) was purchased from Sigma (St. Louis, MO, USA). Lipids were solubilized in chloroform and used without further purification. Skin ceramides (sCer) were extracted from porcine epidermis, which was prepared by heat striping (Kligman and Christophers, 1963) fresh full thickness porcine skin. The SC was obtained following incubation of the epidermis in 0.1% trypsin solution containing 0.5% sodium bicarbonate for 18 h at  $37\text{ }^\circ\text{C}$  and cut into small pieces. The skin lipids were extracted according to the method by Bligh and Dyer (1959) and taken up in chloroform. The sCer was purified from this extract on a silica gel column (60 mesh, 32 cm long, 2.5 cm diameter) with the solvent system as described by Bouwstra et al. (1996). Five milliliter fractions were collected. The presence of ceramides was assessed using thin layer chromatography (Whatman, Silica Gel  $60\text{ }\text{Å}$ ,  $250\text{ }\mu\text{m}$ ). The plates were developed first to the top in chloroform/methanol/acetic acid (90:90:1) and then to the top in diethyl ether/acetic acid (99:1) (McIntosh et al., 1996). Bands were visualized with iodine vapor. All fractions containing sCer were combined and dried in a rotary evaporator and any trace solvent was removed in a vacuum dessicator. Lipids were quantified by weight, taken up in chloroform and stored at  $-20\text{ }^\circ\text{C}$  under  $\text{N}_2$  atmosphere. Their average molecular weight was approximated with  $700\text{ g/mol}$ .

For the ILM model the lipids were mixed in glass vials to achieve molar ratios of SA/Chol/sCer 1:1:1. DMPS was added as 16.5% of the total lipid content for the samples containing

DMPS; the final cumulative lipid concentration was 5 mg/mL. Anodisc inorganic membrane filters (Whatman International Ltd., Maidstone, UK) were used as a support for the ILM model. A small drop of the ILM lipid mixture was applied to the filters, which were then left to dry in air. This procedure was repeated five times on each side. Filters were stored at 4 °C until used.

## 2.6. Transmission FTIR measurements

Empty filters were used to record the background. Occluded filters were hydrated in PBS at 69 °C for 10 s and then placed on a CaF<sub>2</sub> crystal with one side exposed to air. IR-spectra were obtained using a System 2000 IR-Spectrophotometer (Perkin-Elmer). The software Timebase (Perkin-Elmer) was used to collect the data and calculate the areas under the spectra between 2280 and 1900 cm<sup>-1</sup> and between 2913.6 and 2923.6 cm<sup>-1</sup> as a function of time. Averages of 50 spectra were recorded at 3 min intervals over the course of 90 min. Excel (Microsoft) was used to process the time profiles of the hydration band.

## 3. Results and discussion

### 3.1. The effect of DMPS on the hydration of full thickness porcine skin

In this study we determined the hydration of skin pulsed with 4 mg/mL DMPS dispersion and compared it to three controls: skin pulsed with PBS, skin that was not pulsed and exposed to DMPS dispersion and skin that was not pulsed and exposed to PBS. As a reference the water content of untreated ‘dry skin’ was used, i.e., skin that had been kept at controlled 43% RH for a minimum of 30 min and never been treated with donor solution and/or electroporated. The water content in the samples was determined by ATR-FTIR-spectroscopy at four different time points after treatment: immediately and also after 15, 30 or 60 min. For this the weak combination band near 2100 cm<sup>-1</sup> was considered and the area under the peak obtained by integration from 2280 to 1900 cm<sup>-1</sup>. The integrated area under the peak was compared with the background between zero baseline and the baseline of the peak. This procedure removes the effect of scattered radiation caused by different degrees of contact between the sample and the crystal during different runs and provides a quantitative measure of water concentration (Potts et al., 1985).

Fig. 1 shows the relative water content of the SC as it was determined from area under the combination band near 2100 nm<sup>-1</sup>. Four different treatments were studied representing the possible combinations of use or absence of electroporation and DMPS. As a control the hydration of skin that was never exposed to any fluid, ‘dry’ skin, was recorded. The measurements were taken at four different time points after the donor liquid was removed: 0, 15, 30 and 60 min.

Compared to the ‘dry’ samples all treated samples show an increase in hydration immediately after the donor liquid is removed. Fifteen minutes after treatment the unpulsed samples show a decrease in water content to almost that of dry skin. The pulsed samples lose water at a much slower rate. This is in agreement with studies that showed an increase in SC-hydration

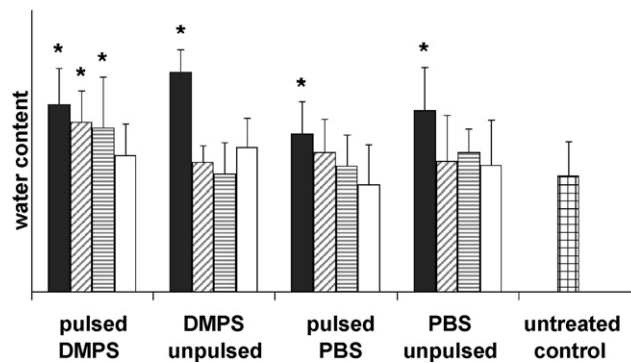


Fig. 1. Hydration, as determined from the area under the IR absorbance peak around 2100 cm<sup>-1</sup>, of pulsed or unpulsed porcine SC after exposure to PBS or DMPS dispersion for 4 min and waiting time in a 43% RH chamber for (■) 0 min, (▨) 15 min, (▩) 30 min or (□) 60 min and (▤) porcine SC that was not exposed to any fluid. Water content is given in arbitrary units. Error bars correspond to standard deviation. (Student's *t*-test was used to determine statistically significant changes with respect to untreated control and “\*” indicates statistically significant difference ( $p < 0.05$ ) from the untreated control.)

after the application of a low voltage potential (Jadoul et al., 1996). Pulsing and even a low voltage electrical current may create water pools within the SC, which cannot evaporate easily. Structural rearrangement within the SC as observed after electroporation (Gallo et al., 1999) are likely to be responsible for this phenomenon. It is interesting to note that there is no statistically significant difference in the initial water content between all treated samples and is most plausibly due to a film of water that remains on the skin after it is exposed to the lipid dispersion or PBS. In ATR-FTIR only the water that is present on the outer layer, the top ~1 μm of the skin surface contributes to the measured absorbance. This layer of adsorbed water evaporates rapidly (within the first 15 min) after the skin is transferred in the constant humidity chamber. The water content determined at the latter time points ( $\geq 15$  min) indicate a migration of water present deeper in the SC to the surface.

The second observation that can be made is that DMPS appears to give the SC a greater capacity for water uptake than PBS alone. Therefore, skin pulsed in the presence of DMPS shows greater hydration at later post-pulse times that cannot be replicated in the absence of electroporation or by pulsing with PBS alone.

Since the standard deviation is fairly large, the significance of the differences between treated samples and dry skin was assessed using Student's *t*-test with a 97.5% confidence level. This method compares the inter-sample and intra-sample variances. We assumed the variances within the groups to be comparable for all treatments since all data points were obtained using the same technique. Fig. 2 shows the differences between the calculated *T*-value, which can be interpreted as a signal-to-noise ratio of the compared data groups, and the tabulated  $t_{crit}$ -value, which marks the value of the distribution of these calculated *T*-values that has a 2.5% probability of occurring randomly. For  $T - t_{crit} > 0$  the water content of the treated sample is significantly different from that of dry skin. The greater  $T - t_{crit}$ , the smaller the probability that the increase in hydration detected would have occurred by chance. For  $T - t_{crit} < 0$

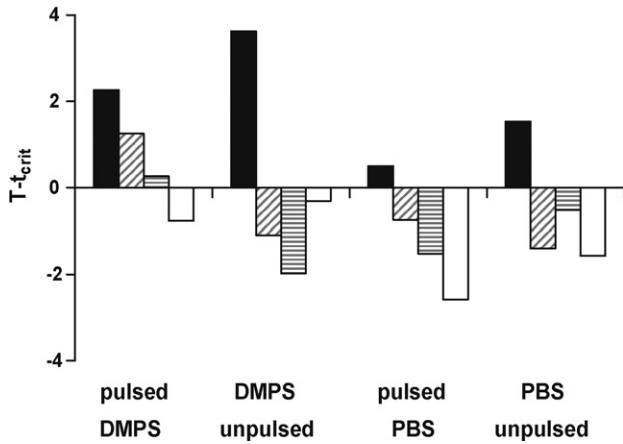


Fig. 2. Results from a  $t$ -test with  $p=0.05$  to determine the significance of the hydration increase in the treated samples over untreated 'dry' control. Shown are the differences  $T - t_{crit}$ , where a positive value indicates that the difference between treated and untreated is significant at a 97.5% confidence level. Hydration was measured at four time points after treatment: (■) 0 min, (▨) 15 min, (▩) 30 min or (□) 60 min.

the water content of the treated sample cannot be said to be significantly different from that of dry skin at a 97.5% confidence level.

As can be determined from Fig. 2, at 15 min after treatment only the sample pulsed with DMPS has a significantly higher degree of hydration than dry SC. This difference is still significant at the 30 min time point; whereas all other samples approach the hydration status of dry SC at 15 min.

### 3.2. Hydration of membranes occluded with ILM model

To determine the hydration behavior of the ILM model, we supported the ILM model inside Anodisc inorganic membrane filters. Diffusion coefficients of water in dimyristoylphosphatidylcholine (DMPC) lipid structures were shown to lie between  $4 \times 10^{-8}$  and  $8 \times 10^{-6}$  cm<sup>2</sup>/s at room temperature (Wästerby et al., 2002). This would result in  $0.019 \text{ s} \leq t_{lag} \leq 37.5 \text{ s}$  for half of our membrane thickness. The diffusion time of water into our membrane model will lie in between these values, since on the one hand the ILM model lipids we used have a tighter packing ( $0.371 \text{ nm} \leq d \leq 0.412 \text{ nm}$ ) (determined from X-ray diffraction studies, unpublished), than DMPC ( $0.409 \text{ nm} \leq d \leq 0.425 \text{ nm}$ ) (Tristram-Nagle et al., 2002) but on the other hand hydration was achieved at a much higher temperature than room temperature. Therefore, we chose to hydrate our model with PBS for 10 s at 69 °C and we expect to have an equilibrated and mostly saturated hydration profile with this treatment at the beginning of our experiments.

In order to evaporate from the membrane, water molecules have to diffuse through the lipids and to the surface. If sink conditions apply and if the sample has a uniform water distribution at the start of the experiment, the water content in the sample,  $w$ , over time,  $t$ , and at any position,  $x$ , can be described by Eq. (1) with the boundary and initial conditions Eqs. (2a)–(2c):

$$w_t(x, t) = Dw_{xx}(x, t), \quad (0 < x < h, t > 0) \quad (1)$$

$$w(x, 0) = w_0, \quad (0 < x < h) \quad (2a)$$

$$-Dw_x(0, t) = 0, \quad (t > 0) \quad (2b)$$

$$-Dw_x(h, t) = kw(h, t), \quad (t > 0) \quad (2c)$$

Here  $D$  is the diffusion coefficient of water in the membrane,  $k$  the rate constant for the evaporation from the surface and  $h$  is the membrane thickness.

The solution to this partial differential equation and boundary as well as initial conditions is described in the appendix. It has the following form:

$$w(x, t) = w_0 h \sum_{n=1}^{\infty} E_n \exp\left(-\gamma_n^2 \frac{h^2}{D} t\right) \cos(\gamma_n x) \quad (3)$$

$$\text{where } E_n \text{ satisfies: } E_n = \frac{2 \sin(\gamma_n)}{\gamma_n + \sin(\gamma_n) \cos(\gamma_n)} \quad (4)$$

$$\text{and } \gamma_n \text{ is determined by: } \tan(\gamma_n) = \frac{(kh)/D}{\gamma_n} \quad (5)$$

$w_0$  is the initial water content. The total water content in the membrane would then be given by Eq. (6):

$$\int_{x=0}^h w(x, t) dx = w_0 h \sum_{n=1}^{\infty} E_n \exp\left(-\gamma_n^2 \frac{h^2}{D} t\right) \frac{\sin(\gamma_n)}{\gamma_n} \quad (6)$$

### 3.3. The effect of DMPS on the water evaporation kinetics from membranes occluded with ILM models

The water content over time was recorded by transmission FTIR-spectroscopy by monitoring the area under the spectra between 2280 and 1900 cm<sup>-1</sup>. To correct for fluctuations in the beam intensity and lipid content of the sample we also monitored the area under the peak for asymmetric CH<sub>2</sub>-stretching vibrations (Bellamy, 1954) between 2913.6 and 2923.6 cm<sup>-1</sup> as a function of time. The lipid content of the filters is constant throughout the experiment.

The area,  $A_L$ , of this lipid band is dependent on the water content of the sample, since the OH-stretching vibration, which absorbs near 3500 cm<sup>-1</sup> (Bellamy, 1954), has a very broad band in these samples. Therefore,  $A_L$  is proportional to the amount of water in the sample,  $w$ , the amount of lipid in the sample,  $l$ , and its size depends on the beam intensity by some factor,  $\alpha$  Eq. (7):

$$A_L = \alpha(k_1 l + k_2 w) \quad (7)$$

The area of the water combination band,  $A_w$ , is proportional to  $w$  and, again, its size is modified to the same extent by the beam intensity as  $A_L$  Eq. (8):

$$A_w = \alpha k_3 c_w \quad (8)$$

$k_1$ ,  $k_2$  and  $k_3$  are the proportionality constants. The ratio of the areas of these two bands at any time point can, therefore, be written as follows:

$$\frac{A_w}{A_L} = \frac{1}{\beta(1/w) + \delta} \quad (9a)$$

where

$$\beta = \frac{k_1}{k_3} \quad (9b)$$

and

$$\delta = \frac{k_2}{k_3} \quad (9c)$$

This treatment did not change the overall shape of the data and in particular did not lengthen the duration of the initial slow intensity decrease. Therefore,  $\delta$  can be assumed to be negligible and only the data normalized to the lipid content will be discussed.

The shape of the evaporation profiles is characterized by two time constants. The initial evaporation for both treatments is fairly slow. After a certain time, however, the water content drops off rapidly. Cooperativity for the hydration of lipid layers has been reported for different phospholipids and can be attributed to conformational changes of the headgroups upon hydration (Miller and Bach, 1999). Very high water content can also lead to the disruption of the lipid arrangement. This means that the rate of water loss from the sample,  $k$ , as well as the diffusivity of water in the lipid layers,  $D$ , can be expected to vary with the water concentration in the membrane. The following scenarios may occur:

- If  $k$  or  $D$  are concentration dependent, a very complex boundary condition results in Eq. (2c), which prohibits the evaluation of the system.
- If  $k$  or  $D$  are step functions with constant value for different ranges of  $c_w$ , the solution given in Eq. (6) holds. In this case,  $\gamma_n$  would have to be determined for each  $k$  or  $D$  value. Mathematical simulations show that, e.g. a 100-fold increase in  $k$  at a critical concentration may produce similar concentration kinetics as were seen in our data (results not shown). Exact solutions cannot be determined since exact values for  $k$  and  $D$  are unknown, which prohibits the determination of  $\gamma_n$  and, hence, the fit of the data.

The initial slow time constant of the water loss followed by the fast time constant suggests that a conformation change of the lipids upon dehydration results in either faster diffusion or faster evaporation or both. This suggests that the water binding regions are fully saturated at that point.

The initial ratio of water/lipid is significantly greater in the sample with the potential enhancer ( $p \leq 0.001$ ). The time, after which the water loss from the sample becomes very rapid, is generally in a similar range for the sample containing DMPS and for the sample without the potential enhancer (Fig. 3), about 1800 s. This suggests that DMPS does not prolong the water retention time of ILM models. However, DMPS increases their capacity for water uptake. Still, a higher initial hydration results in an elevated hydration status at later times following the removal of the hydrating agent if the evaporation rates are the same.

The increased and prolonged hydrated state of the SC following electroporation in the presence of DMPS may help partially explain the previously observed increased transdermal transport of solutes since the partition coefficient and permeability are

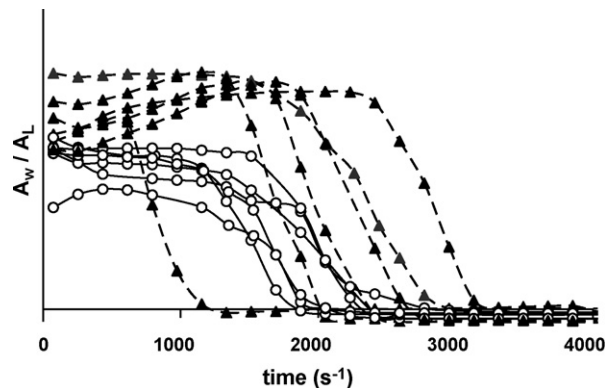


Fig. 3. Normalized water content of hydrated ILM models exposed to dry air over time, calculated as the ratio of  $A_w$ , the area under the water peak near  $2100 \text{ cm}^{-1}$ , to  $A_L$ , the area under the lipid peak at  $2919 \text{ cm}^{-1}$ . (—▲—) ILM model containing 16.5% DMPS (—○—) ILM model containing no DMPS.

likely to be increased. In a related study (unpublished) using the same aluminum oxide (Anodisk) filters occluded using the SC ILM model and carboxyfluorescein (CF) as a model solute we found that DMPS when added to ILM model increased the partition coefficient for CF by a factor of 6 and increased the permeability by a factor of 5.

#### 4. Conclusions

The data presented here show that electroporation of full thickness porcine skin with DMPS leads to greater hydration of the SC for longer periods of time. The results from studies of the ILM model suggest that this is caused by the increased hydration capacity of the ILM in the presence of DMPS.

#### Acknowledgements

We thank Dr. Johannes Nitsche, Department of Chemical Engineering SUNY Buffalo, NY, USA, for his input in this study and for critically reading the manuscript and we also thank Dr. John Canty, Center for Cardiovascular Research, SUNY Buffalo, NY, USA, for the porcine skin. This work is supported by a grant EB 001034 from the National Institutes of Health and the Institute core grant CA016156 from the National Cancer Institute.

#### Appendix A

Notes on solving the partial differential equation for the description of the kinetics of water evaporation the SC filter model.

To simplify, the following dimensionless parameters were introduced:

$$\hat{w} = \frac{w}{w_0}, \quad \hat{x} = \frac{x}{h}, \quad \hat{t} = \frac{tD}{h^2}, \quad \beta = \frac{kh}{D}$$

Substitution of these dimensionless parameters into Eq. (1) and (2a)–(2c) leads to:

$$\frac{\partial \hat{w}}{\partial \hat{t}} = \frac{\partial^2 \hat{w}}{\partial \hat{x}^2} \quad (A1)$$

$$\hat{w}(\hat{x}, 0) = 1 \quad (\text{A2})$$

$$\left. \frac{\partial \hat{w}}{\partial \hat{x}} \right|_{\hat{x}=0} = 0 \quad (\text{A3})$$

$$\left. \frac{\partial \hat{w}}{\partial \hat{x}} \right|_{\hat{x}=1} = \frac{kh}{D} \hat{w} = \beta \hat{w} \quad (\text{A4})$$

Eq. (A1) has a solution of the form:

$$\hat{w} = f(\hat{x})g(\hat{t}) \quad (\text{A5})$$

Substitution of Eq. (A5) into Eq. (A1) gives the following relationship:

$$\frac{dg/d\hat{t}}{g} = \frac{d^2 f/d\hat{x}^2}{f} = -\alpha \quad (\text{A6})$$

$\alpha$  is a constant. For  $\alpha < 0$  the solution would be exponentially growing in time, which will become obvious further down Eq. (A15) and for  $\alpha = 0$  no change over time would happen at all. Since these are not physically reasonable assumptions,  $\alpha > 0$  and we can set:

$$\alpha = \gamma^2 \quad (\text{A7})$$

Considering the second term of Eq. (A6), it follows from Eqs. (A1)–(A4) that:

$$\frac{d^2 f}{d\hat{x}^2} + \gamma^2 f = 0 \quad (\text{A8})$$

$$\left. \frac{df}{d\hat{x}} \right|_{\hat{x}=0} = 0 \quad (\text{A9})$$

$$-\left. \frac{df}{d\hat{x}} \right|_{\hat{x}=1} = \beta f(1) \quad (\text{A10})$$

The solution to Eq. (A8) has the form:

$$f = A \cos(\gamma \hat{x}) + B \sin(\gamma \hat{x}) \quad (\text{A11})$$

and the first derivative is given by:

$$\frac{df}{d\hat{x}} = -A\gamma \cos(\gamma \hat{x}) + B\gamma \sin(\gamma \hat{x}) \quad (\text{A12})$$

Eqs. (A9) and (A12) determine that  $B = 0$  and, therefore, Eq. (A10) determines the following relationship:

$$\frac{\sin(\gamma)}{\cos(\gamma)} = \tan(\gamma) = \frac{\beta}{\gamma} \quad (\text{A13})$$

There are  $n$  solutions  $\gamma_n$  to this equation, where  $0 < \gamma_n < 1/2\pi$  for  $n = 1$  and  $(n - 1)\pi < \gamma_n < (n - 1/2)\pi$  for  $n \geq 2$ .

The left term of Eq. (A6) has the following form if the substitution (A7) is made:

$$\frac{dg}{d\hat{t}} = -\gamma^2 g \quad (\text{A14})$$

The general solution to this differential equation is exponential:

$$g = E \exp(-\gamma^2 \hat{t}) \quad (\text{A15})$$

$E$  is a parameter. Combining Eqs. (A14) and (A11) into Eq. (A5), the solution to the partial differential equation Eq. (A1) is given by:

$$\hat{w}(\hat{x}, \hat{t}) = \sum_{n=1}^{\infty} E_n \exp(-\gamma_n^2 \hat{t}) \cos(\gamma_n^2 \hat{x}) \quad (\text{A16})$$

The initial condition Eq. (A2) requires that

$$\hat{w}(\hat{x}, 0) = \sum_{n=1}^{\infty} E_n \cos(\gamma_n^2 \hat{x}) = 1 \quad (\text{A17})$$

which allows the determination of the parameters  $E_n$ :

$$E_n = \frac{\int_0^1 1 \cos(\gamma_n \hat{x}) d\hat{x}}{\int_0^1 (\cos(\gamma_n \hat{x}))^2 d\hat{x}} = \frac{2 \sin(\gamma_n)}{\gamma_n + \sin(\gamma_n) \cos(\gamma_n)} \quad (\text{A18})$$

The water content in the entire membrane volume can be determined by integrating Eq. (A17) over the space coordinate between 0 and 1:

$$\int_0^1 \hat{w}(\hat{x}, \hat{t}) d\hat{x} = \sum_{n=1}^{\infty} E_n \exp(-\gamma_n^2 \hat{t}) \frac{1}{\gamma_n} \sin(\gamma_n) \quad (\text{A19})$$

Therefore, the absolute water content in the sample can be obtained if the initial substitutions are reversed:

$$\int_0^h w(x, t) dx = w_0 h \sum_{n=1}^{\infty} E_n \exp(-\gamma_n^2 t) \frac{1}{\gamma_n} \sin(\gamma_n) \quad (\text{A20})$$

## References

- Bellamy, L.J., 1954. The Infra-red Spectra of Complex Molecules. John Wiley & Sons Inc., New York.
- Blank, I.H., 1951. Factors which influence the water content of the stratum corneum. *J. Invest. Dermatol.* 18, 433–440.
- Bligh, E.G., Dyer, W.J., 1959. A rapid method of total lipid extraction and purification. *Can. J. Biochem. Phys.* 37, 911–917.
- Bouwstra, J.A., Gorris, G.S., Cheng, K., Weerheim, A., Bras, W., Ponc, M., 1996. Phase behavior of isolated skin lipids. *J. Lipid Res.* 37, 999–1011.
- Cronin, E., Stoughton, R.B., 1962. Percutaneous absorption. Regional variations and the effect of hydration and epidermal stripping. *Br. J. Dermatol.* 74, 265–272.
- Edwardson, P.A.D., Walker, M., Gardner, R.S., Jacques, E., 1991. The use of FT-IR for the determination of stratum corneum hydration in vitro and in vivo. *J. Pharmaceut. Biomed.* 9, 1089–1094.
- Feldmann, R.J., Maibach, H.I., 1974. Percutaneous penetration of hydrocortison with urea. *Arch. Dermatol.* 109, 58–59.
- Gallo, S.A., Sen, A., Hensen, M.L., Hui, S.W., 1999. Time-dependent ultra-structural changes to porcine stratum corneum following an electric pulse. *Biophys. J.* 76, 2824–2832.
- Greenspan, L., 1977. Humidity fixed points of binary saturated aqueous solutions. *J. Res. NBS A Phys.*, 89–96 (Chapter 81A).
- Jadoul, A., Doucet, J., Durand, D., Preat, V., 1996. Modifications induced on stratum corneum structure after in vitro iontophoresis: ATR-FTIR and X-ray scattering studies. *J. Controlled Release* 42, 165–173.
- Jadoul, A., Bouwstra, J.A., Preat, V., 1999. Effects of iontophoresis and electro-poration on the stratum corneum. Review of the biophysical studies. *Adv. Drug Deliv. Rev.* 35, 89–105.
- Kligman, A.M., Christophers, E., 1963. Preparation of isolated sheets of human stratum corneum. *Arch. Dermatol.* 88, 702–705.
- McIntosh, T.J., Stewart, M.E., Downing, D.T., 1996. X-ray diffraction analysis of isolated skin lipids: reconstitution of intercellular lipid domains. *Biochemistry-US* 35, 3649–3653.

- Miller, I.R., Bach, D., 1999. Hydration of phosphatidyl serine multilayers and its modulation by conformational change induced by correlated electrostatic interaction. *Bioelectrochem. Bioenerg.* 48, 361–367.
- Potts, R.O., Guzek, D.B., Harris, R.R., McKie, J.E., 1985. A noninvasive, in vivo technique to quantitatively measure water concentration of the stratum corneum using attenuated total-reflectance infrared spectroscopy. *Arch. Dermatol. Res.* 277, 489–495.
- Scheuplein, R.J., Ross, L.W., 1974. Mechanism of percutaneous absorption. V. Percutaneous absorption of solvent deposited solutes. *J. Invest. Dermatol.* 62, 353–360.
- Sen, A., Zhao, Y.L., Zhang, L., Hui, S.W., 2002a. Enhanced transdermal transport by electroporation using anionic lipids. *J. Controlled Release* 82, 399–405.
- Sen, A., Zhao, Y.L., Hui, S.W., 2002b. Saturated anionic phospholipids enhance transdermal transport by electroporation. *Biophys. J.* 83, 2064–2073.
- Sen, A., Daly, M.E., Hui, S.W., 2002c. Transdermal insulin delivery using lipid enhanced electroporation. *BBA-Biomembranes* 1564, 5–8.
- Tristram-Nagle, S., Liu, Y., Legleiter, J., Nagle, J.F., 2002. Structure of gel phase DMPC determined by X-ray diffraction. *Biophys. J.* 83, 3324–3335.
- Walters, K.A., 1989. Penetration enhancers and their use in transdermal therapeutic systems. In: Hadgraft, J., Guy, R.H. (Eds.), *Transdermal Drug Delivery—Developmental Issues and Research Initiatives*. Marcel Dekker Inc., New York and Basel, pp. 197–246.
- Warner, R.R., Stone, K.J., Boissy, Y.L., 2003. Hydration disrupts human *stratum corneum* ultrastructure. *J. Invest. Dermatol.* 120, 275–284.
- Wästerby, P., Orädd, G., Lindblom, G., 2002. Anisotropic water diffusion in macroscopically oriented lipid bilayers studied by pulsed magnetic field gradient NMR. *J. Magn. Reson.* 157, 156–159.
- Williams, A., 1995. Urea and its derivatives as penetration enhancers. In: Smith, E.W., Maibach, H.I. (Eds.), *Percutaneous Penetration Enhancers*. CRC Press, Boca Raton, New York, London and Tokyo, pp. 289–307.